

# THE 4TH INTERNATIONAL CONFERENCE ON ALUMINUM ALLOYS

## AGE HARDENING AND PRECIPITATION IN AN Al-Al<sub>2</sub>O<sub>3</sub> BASED METAL MATRIX COMPOSITE

G.A. Edwards<sup>1</sup>, M.J. Couper<sup>2</sup> and G.L. Dunlop<sup>1</sup>

1. CRC for Alloy and Solidification Technology (CAST), Department of Mining and Metallurgical Engineering, The University of Queensland, St. Lucia, Queensland, AUSTRALIA 4072.
2. Comalco Research Centre, 15 Edgars Rd., Thomastown, Victoria, AUSTRALIA 3074.

### Abstract

The development of microstructure in Al alloy 6061 and Comral-85<sup>TM</sup> composite has been compared using transmission electron microscopy (TEM). It was found that a higher density of dislocations in the composite material accelerated precipitation during artificial ageing. Dislocations accelerated the growth of  $\beta''$ , the  $\beta''$  to  $B'$  transformation and the subsequent growth of  $B'$ . The density of precipitates that had nucleated on dislocations was highest close to the ceramic reinforcement in the composite material. The relationship between these microstructural observations and differences in the age hardening behaviour of the two materials is discussed.

### Introduction

Previous work has shown that age hardening and precipitation is accelerated in Al-Mg-Si alloy-based metal matrix composites (MMCs) compared to unreinforced alloys [1-11]. This has been attributed to increased dislocation densities in the composites [2-10]. It has been proposed that dislocations accelerate the formation and growth of precipitates, which affects the age hardening behaviour of MMCs. It has also been found that age hardening may be inhibited in some MMCs, and it has been suggested that this may be due to loss of quenched-in vacancies [12,13] or loss of Mg to ceramic/molten alloy reactions that occur during melt processing [14-16].

However precipitation in MMCs has generally been poorly characterised. Presumably this is due to difficulties in preparing high quality thin foils for investigation by TEM. In particular, the detailed relationship between microstructural features in MMCs and age hardening and DSC results for the materials has not been clearly established.

In this investigation, the development of microstructure in Comral-85 composite and alloy 6061 during age hardening is compared. Comral-85 composite contains ceramic microspheres (average diameter  $\sim 20\mu\text{m}$ ) that are embedded in an Al alloy 6061 matrix. The microspheres consisted mainly of mullite ( $3\text{Al}_2\text{O}_3 \cdot 2\text{SiO}_2$ ) and corundum ( $\alpha\text{Al}_2\text{O}_3$ ) grains. Previous investigations [1] have shown that age hardening is accelerated in Comral-85 composite compared to the case for unreinforced alloy 6061, during both isothermal ageing and air cooling from solution treatment. A layer of  $\text{MgAl}_2\text{O}_4$  spinel and occasional  $\alpha\text{-AlFeSi}$  precipitates have been found to form at the ceramic/matrix interface in Comral-85 composite that had been melt processed [1,17], however neither phase directly affected precipitation in the alloy matrix.

## Experimental

Comral-85 composite and Al alloy 6061 were supplied by Comalco Research Centre in the form of as-extruded bar. The composition of the composite matrix was: 0.82Mg, 0.79Si, 0.20Cu, 0.20Fe, 0.10Ti, and that of the alloy 6061 was: 0.80Mg, 0.79Si, 0.18Cu, 0.22Fe, 0.01Ti. Specimens were solution treated for 1.5h at 530°C, water quenched and then immediately isothermally aged.

Thin-foil specimens for TEM were prepared from alloy 6061 by electropolishing in a nitric acid:methanol 1:4 solution, at -30°C and ~8V, using a Tenupol jet polisher. Specimens from Comral-85 composite were also prepared using this technique. These specimens contained electron transparent regions in the alloy matrix away from the interface, however areas that were close to the microspheres were generally quite thick. Specimens that contained thin regions in both the ceramic and the alloy matrix were prepared by ion beam thinning at low angles (~2-3°). TEM was performed using JEOL 4000FX and 1210 instruments, operating at 400kV and 120kV respectively.

High resolution dark-field electron microscopy (HRDEM) was used to identify the crystal structures of individual fine-scale precipitates. This technique has not been extensively used previously, due to difficulties in the interpretation of the images and the possibility of false detail appearing in the images [18]. However, by using a small objective aperture that contains several precipitate reflections, it is possible to obtain an image that contains periodicities matching those of the crystal structure [18]. In this investigation the technique was used with care, to identify precipitates whose crystal structures had previously been identified by other means. The images were obtained by aligning the beam with  $\langle 001 \rangle_{Al}$ , and then tilting the beam to position a small objective aperture between the strong Al reflections, as shown in Figure 1.

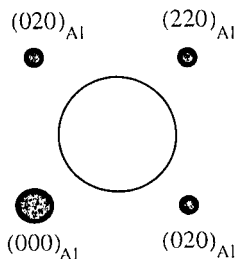


Figure 1. Schematic diagram showing the position of the objective aperture for high resolution dark-field imaging. The beam was aligned with  $\langle 001 \rangle_{Al}$ , and tilted illumination was used to position the aperture between the Al reflections.

## Age Hardening

Age hardening curves that were obtained by artificially ageing Comral-85 composite and alloy 6061 at 175°C are presented in Figure 2. The age hardening in the early to peak stages of ageing is slightly accelerated in the composite compared to alloy 6061. However this is only a small effect. The peak in hardness for the composite occurred after ~4h ageing, whereas for alloy 6061 the peak occurred after ~8h ageing. The most significant difference in the age hardening results was a significantly more rapid overageing in Comral-85 composite.

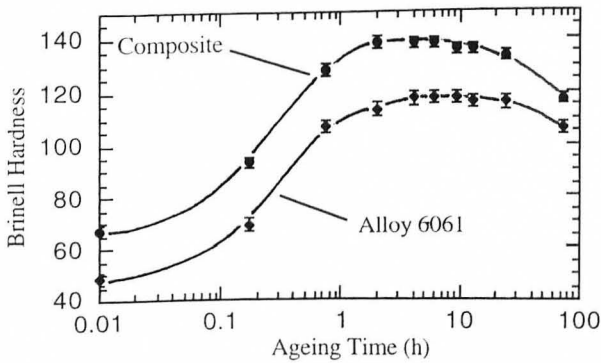
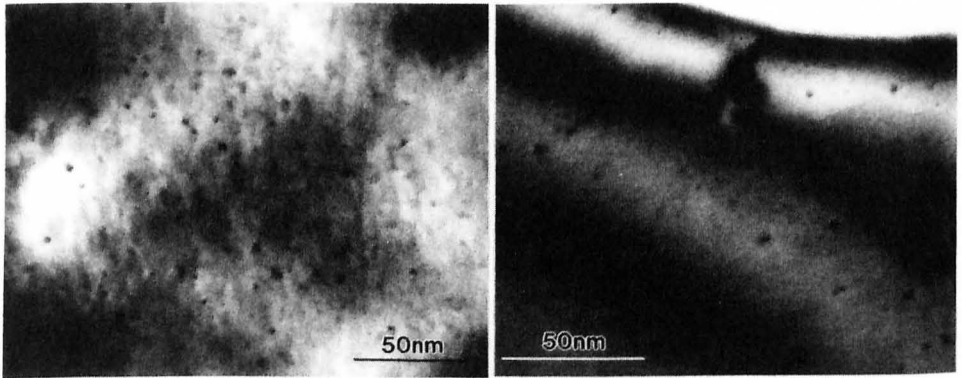


Figure 2. Age hardening curves for alloy 6061 and Comral-85 composite after ageing at 175°C. The most significant difference was the more rapid overaging in the composite material compared to alloy 6061.

#### TEM Analysis of Microstructure

Figure 3 shows TEM bright field micrographs of the matrix in Comral-85 composite and alloy 6061 that had been aged for 10 minutes at 175°C. This ageing treatment corresponds to an underaged condition (Figure 2). Both materials contained small precipitates of unknown structure [19] and there was little obvious difference in the microstructures.



(a)

(b)

Figure 3. TEM bright field micrographs of (a) alloy 6061 and (b) the alloy matrix in Comral-85 composite that had been aged for 10 minutes at 175°C. Both materials contained small precipitates of unknown structure.

The microstructures in the alloy matrix of Comral-85 composite and in alloy 6061 were also similar after ageing close to peak hardness (Figure 4). The predominant precipitate was  $\beta''$  [19]. However dark-field micrographs that were obtained with the objective aperture in the position shown in Figure 1 highlighted a significant number of lath-shaped precipitates that had formed close to the ceramic/matrix interfaces in Comral-85 composite (Figure 5(a)). The precipitates had formed along definite lines, indicating that they had nucleated on dislocations. Dark-field images that were

obtained with  $B=[013]_{Al}$  highlighted needle-shaped precipitates that were perpendicular to the beam (Figure 5(b)). The image in Figure 5(b) was obtained by selecting the arrowed streak in the SADP. Homogeneously nucleated  $\beta''$  precipitates were visible in such images and were approximately 15nm long (Figure 6). However there was also a significant number of much longer precipitates (~75nm) close to the ceramic/matrix interfaces. The fact that there were more of these precipitates close to the interface suggest that they are the lath-shaped precipitates that are imaged in cross-section in Figure 5(a).

High resolution dark-field micrographs showed that the crystal structures of these precipitates were very similar to, and perhaps identical to, the structure of  $\beta''$  (Figure 6). In Figure 6, the angle  $\theta$  and the ratio  $a/c$  were very similar to the corresponding values for the  $\beta''$  structure [19]. However the spacing  $t$  was measured as 10.3Å, whereas the corresponding spacing in the  $\beta''$  lattice is 11.6Å. It is not known whether this precipitate did in fact have a slightly different lattice parameter to  $\beta''$ , or whether this difference was due to inaccuracies in the dark-field image. In any case, the precipitate is at least very similar to  $\beta''$ , and would thus be expected to produce significant hardening.

These results indicate that the regions around ceramic microspheres contained a significant number of precipitates that nucleated on dislocations and grew rapidly. The similarity between the crystal structures of these precipitates and  $\beta''$  suggests that the rapid growth of these precipitates might accelerate age hardening.

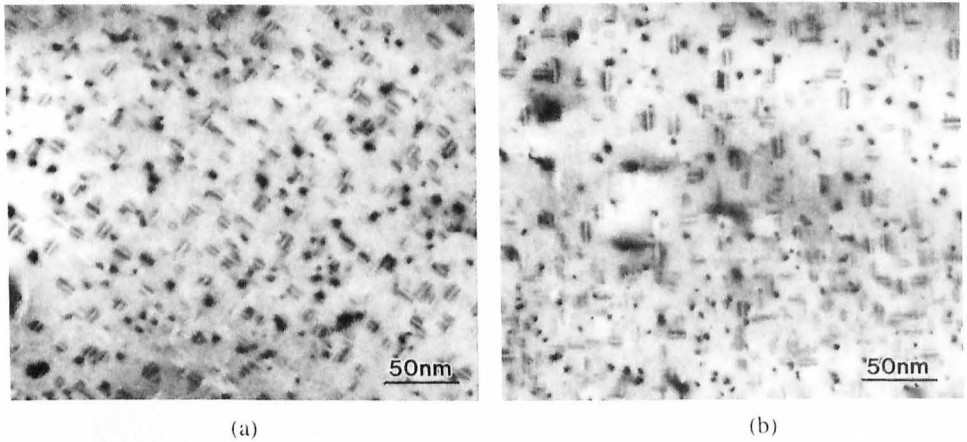
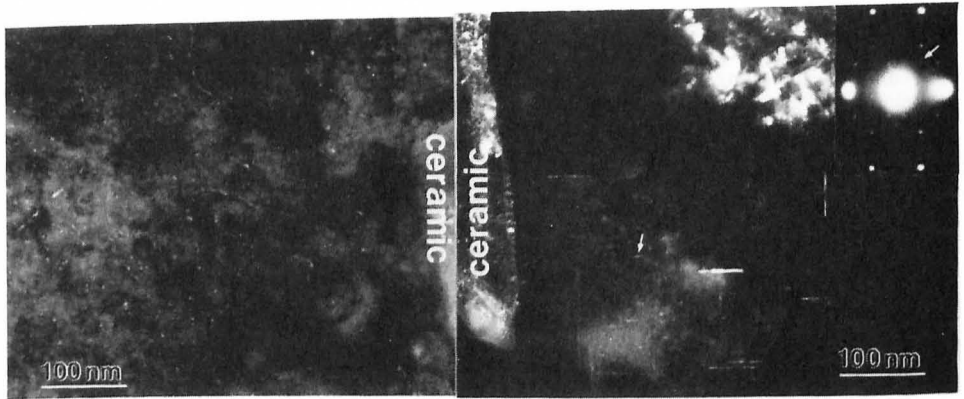


Figure 4. TEM bright field micrographs ( $B = [001]_{Al}$ ) of (a) alloy 6061 and (b) the matrix in Comral-85 composite that had been aged for 4h at 175°C. Both microstructures are similar, mainly consisting of  $\beta''$  precipitates that were approximately 15nm long.



(a) (b)  
 Figure 5. (a) Dark field TEM micrograph ( $B = [001]_{Al}$ ) showing a significant number of lath-shaped precipitates close to a ceramic/matrix interface in Comral-85 composite that had been aged for 4h at 175°C. (b) Dark field micrograph ( $B = [013]_{Al}$ ) that was obtained using the indicated streak on the SADP. There were a significant number of precipitates close to the ceramic/matrix interface that were longer than homogeneously nucleated  $\beta''$  precipitates (arrowed). This suggests that these precipitates are the lath-shaped precipitates that were imaged in cross-section in (a).

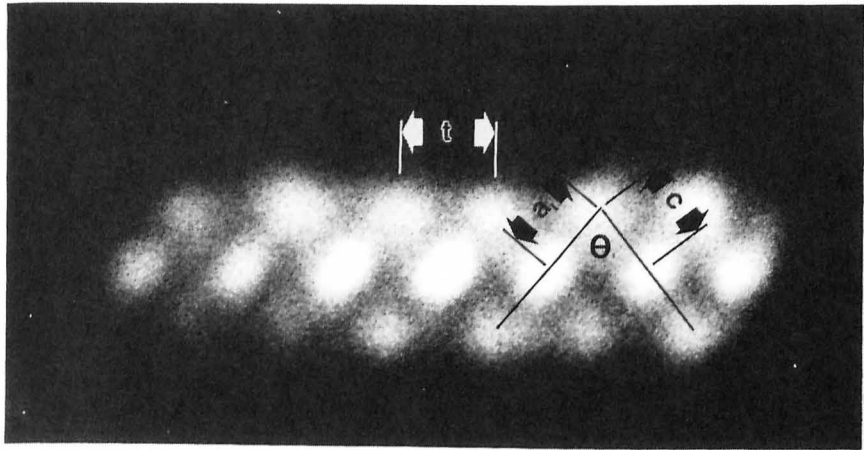


Figure 6. High resolution dark field image of the lath-shaped precipitates in Figure 5 (a). The angle  $\theta$  and the ratio  $a/c$  were similar to that for  $\beta''$ . However the spacing  $t$  was slightly smaller than the corresponding spacing in the  $\beta''$  structure (10.3Å c.f. 11.6Å).

The overaged microstructures in the alloy matrix of the composite and alloy 6061 were substantially different (Figure 7). There were many more long, lath-shaped precipitates in the composite than in alloy 6061. The average length of the lath-shaped precipitates was  $\sim 250$ nm, which is significantly longer than the lath-shaped precipitates that were present after 4h ageing at 175°C ( $\sim 75$ nm). High resolution dark-field images showed that the structure of the precipitates matched the structure of  $B'$  (hexagonal,  $a = 10.4 \text{ \AA}$ ) [19] (Figure 8). Dark-field images showed that similar to the case for lath-shaped precipitates in the specimen that was aged for 4h at 175°C, the number of lath-shaped precipitates was generally higher close to the ceramic microspheres. This is

demonstrated in Figure 9. Figure 9(a) is a dark-field micrograph showing a high number of lath-shaped precipitates close to a ceramic/matrix interface. Figure 9(b) is a similar micrograph from a region that was  $\sim 20\mu\text{m}$  away from the ceramic/matrix interface. Clearly there were very few lath-shaped precipitates away from the interface, where the predominant precipitate was  $\beta''$ . In fact the microstructure in the regions that were far from the interface in Comral-85 composite appeared similar to those in alloy 6061 that had been aged to the same condition (Figure 10).

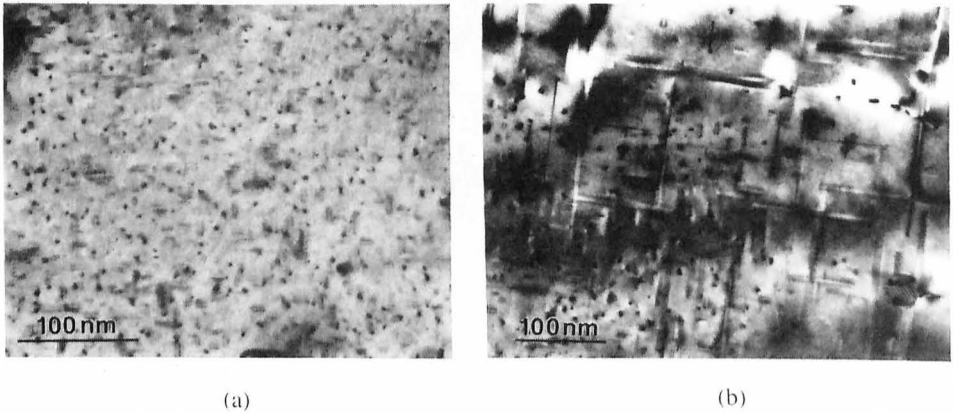


Figure 7. Microstructures after ageing for 72h at  $175^\circ\text{C}$  in (a) alloy 6061, and (b) the matrix in Comral-85 composite. There were significantly more long, lath-shaped precipitates in the composite material.

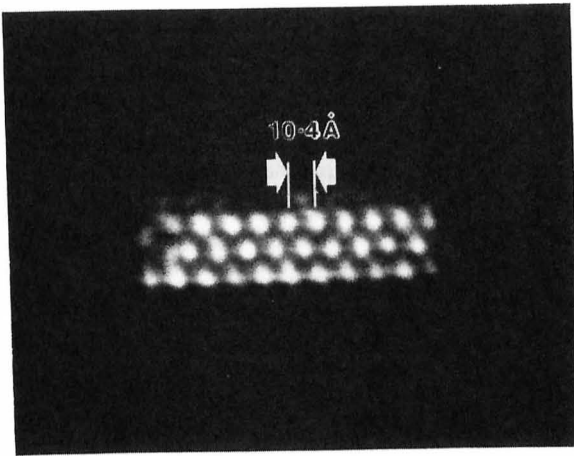


Figure 8. High resolution dark field micrograph of a lath-shaped precipitate in Comral-85 composite that had been aged for 72h at  $175^\circ\text{C}$ . The image matches the structure of  $B'$  (hexagonal,  $a = 10.4\text{\AA}$ ,  $c = 4.05\text{\AA}$ )

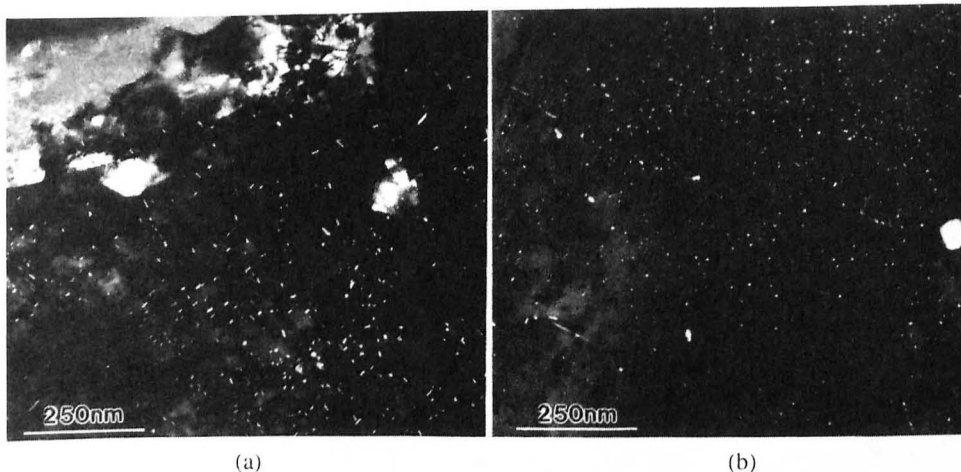


Figure 9. Dark field micrographs showing precipitates in Comral-85 composite that had been aged for 72h at 175°C. (a) Close to a ceramic/matrix interface in Comral-85 composite, and (b) ~20µm away from the interface in (a). There was a higher density of lath-shaped B' precipitates close to the microsphere in Comral-85 composite. Away from the microsphere, the microstructure appeared to be similar to that for alloy 6061 (Figure 10), containing mostly  $\beta''$  precipitates.

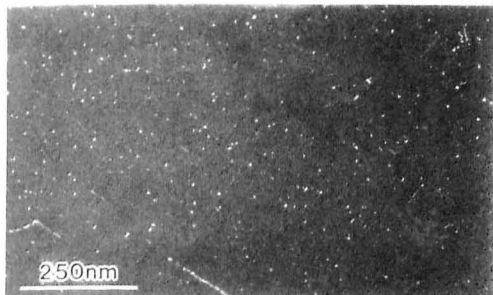


Figure 10. Dark field electron micrograph showing  $\beta''$  precipitates in alloy 6061 that had been aged for 72h at 175°C. The precipitate dispersion appeared to be similar to that in regions that were away from the interface in Comral-85 composite (Figure 9(b)).

### Discussion

The results show that the precipitation sequences in alloy 6061 and Comral-85 composite are similar. The only significant difference in the microstructures of the two materials was the higher density of precipitates that had nucleated on dislocations in Comral-85 composite. The precipitates that nucleated on dislocations grew rapidly as ageing progressed, meaning that the volume of the alloy matrix that was affected by these precipitates increased during ageing. This is in agreement with the ageing curves for alloy 6061 and Comral-85 composite: the difference in the age hardening behaviour of the two materials increased with ageing time. The rapid growth of  $\beta''$  precipitates on dislocations correlates with the slightly accelerated hardening in the composite material that occurred prior to peak hardness. The markedly accelerated overageing in Comral-85 composite, compared to alloy 6061, was associated with the development of a large number of B' precipitates in the alloy matrix of the composite. This indicates that the B' precipitates are not ideal for strengthening. The  $\beta''$  precipitates that had grown from dislocations after 4h ageing at 175°C

must have transformed to B' somewhere between 4h and 72h ageing at 175°C. Thus the  $\beta''$  to B' transformation was significantly accelerated for precipitates that had nucleated on dislocations, since homogeneously nucleated precipitates were not observed to transform to B' at any stage of ageing at 175°C. The exact point at which the precipitates that had formed on dislocations become detrimental to mechanical properties is not known. It was observed that overageing in alloy 6061 at 175°C was associated with a slight coarsening of the  $\beta''$  precipitate dispersion, which suggests that there is an optimum size for the  $\beta''$  precipitates. Therefore the precipitates that nucleate on dislocations probably begin to reduce the strength of the bulk material when they reach a certain size. Obviously this will occur earlier for the precipitates on dislocations than for homogeneously nucleated precipitates. It is to be expected that a further sharp decrease in properties should occur when the  $\beta''$  precipitates that had nucleated on dislocations transform to B'. Inspection of the age hardening curve for Comral-85 composite suggests that this may have occurred after ~20h ageing at 175°C.

The fact that the precipitate dispersions close to the microspheres were significantly different to those further away from the microspheres suggests that it may be difficult to attain optimum microstructures in both regions simultaneously. This would mean that the increase in strength due to artificial ageing would be reduced in the composite material compared to alloy 6061. However, for normal artificial ageing treatments (~8h at 175°C) the difference in the age hardening curves for the two materials was only small, suggesting that the precipitates that nucleated on dislocations did not greatly affect the strength of the composite material at this stage.

#### Acknowledgments

Financial support from Comalco Research Centre is gratefully acknowledged.

#### References

1. G.A. Edwards, J-Y. Yao, M.J. Couper and G.L. Dunlop, Aluminium Alloys: Their Physical and Mechanical Properties, Vol. 1, Eds. L. Arnberg et al., (Norwegian Inst. of Technology and SINTEF Metallurgy, Trondheim, 1992), 525.
2. J.-P. Cottu, J.-J. Couderc, B. Viguier and L. Bernard, J. Materials Science, 27, (1992), 3068.
3. I. Dutta, S.M. Allen and J.L. Hafley, Metallurgical Transactions A, 22A, (1991), 553.
4. P. Appendino, C. Badini, F. Marino & A. Tomasi, Materials Science and Engineering, A135, (1991), 275.
5. D. Dafir, Materials Science and Engineering, A144, (1991), 311.
6. I. Dutta and D.L. Bourell, Acta Metallurgica and Materiala, 38, No. 11, (1990), 2041.
7. I. Dutta and D.L. Bourell, Materials Science and Engineering, A112, (1989), 67.
8. I. Dutta, D.L. Bourell and D. Latimer, J. Composite Materials, 22, (1988), 829.
9. S. Abis & G. Donzelli, J. Materials Science Letters, 7, (1988), 51.
10. G. Nieh and R.F. Karlak, Scripta Metallurgica, 18, (1984), 25.
11. J.M. Papazian, Metallurgical Transactions, 19A, (1988), 2953.
12. S. Ceresara & P. Fiorini, Powder Metallurgy, 24, No. 4, (1981), 210.
13. C.M. Friend and S.D. Luxton, J. Materials Science, 23, 1988, 3173.
14. L. Salvo, M. Suery, J.G. Legoux and G. l'Esperance, Materials Science and Engineering, A135, 1991, 129.
15. Y. Le Petitcorps, J. M. Quenisset, G. Le Borgne and M. Barthole, Materials Science and Engineering, A135, 1991, 37.
16. H. Ribes, M Suery, Scripta Metallurgica, 23, 1989, 705.
17. J-Y. Yao, G.A. Edwards, M.J. Couper and G.L. Dunlop, Aluminium Alloys: Their Physical and Mechanical Properties, Vol. 1, Eds. L. Arnberg et al., (Norwegian Inst. of Technology and SINTEF Metallurgy, Trondheim, 1992), 429.
18. J.M. Cowley, Acta Crystallographica, A29, (1973), 529.
19. G.A. Edwards, G.L. Dunlop and M.J. Couper, this proceedings.